Neuroradiology (2003) 45: 90–94
DOI 10.1007/s00234-002-0898-4

K. Tsuchiya
S. Katase
A. Fujikawa
J. Hachiya
H. Kanazawa
K. Yodo

Diffusion-weighted MRI of the cervical spinal cord using a single-shot fast spin-echo technique: findings in normal subjects and in myelomalacia

Received: 27 September 2002
Accepted: 8 October 2002
Published online: 15 January 2003

K. Tsuchiya (✉) · S. Katase · A. Fujikawa
J. Hachiya
Department of Radiology,
Kyorin University School of Medicine,
6-20-2 Shinkawa, Mitaka,
181-8611 Tokyo, Japan
Email: tsuchiyak-kyr@umin.ac.jp
Tel.: +81-422-475511
Fax: +81-422-760361

H. Kanazawa
Toshiba Corporation,
1-1-1 Shibaura, Minato-ku,
105-8001 Tokyo, Japan

K. Yodo
Toshiba Medical Systems,
3-26-5 Hongo, Bunkyo-ku
113-8456 Tokyo, Japan

Abstract We have implemented a new diffusion-weighted MRI (DWI) sequence based on the single-shot fast spin-echo technique. We hypothesised that this would add information to conventional MRI for diagnosis of lesions of the cervical spinal cord. DWI was performed using a technique in which echo collection after the application of motion-probing gradients was done in the same manner as in the single-shot fast spin-echo technique. We first imaged six healthy volunteers to demonstrate the cervical spinal cord using the sequence. Then we applied the sequence to 12 patients with cervical myelomalacia due to chronic cord compression. The spinal cord was well seen in all subjects without the distortion associated with echo-planar DWI. In the patients, lesions appeared as areas of low- or isointense signal on DWI. Calculated apparent diffusion coefficients of the lesions ($3.30 \pm 0.38 \times 10^{-3}$ mm^2/s) were significantly higher than those of normal volunteers ($2.26 \pm 0.08 \times 10^{-3}$ mm^2/s). Increased diffusion in areas of cervical myelomalacia, suggesting irreversible damage, can be detected using this technique.

Keywords Spinal cord · Myelomalacia · Magnetic resonance imaging · Diffusion

Introduction

Unlike its widespread use in the brain, the application of diffusion-weighted MRI (DWI) to the spinal cord lesions is limited to several reports in which a line scan, a navigated pulsed-gradient-echo technique and a radial scan were used [1, 2, 3]. DWI can be expected to facilitate early diagnosis as well as characterisation of spinal cord disease such as ischaemia, infection, neoplasms and demyelination. Spinal DWI, however, is difficult to obtain because of physiological motion, including the flow of cerebrospinal fluid (CSF). Single-shot echo-planar DWI, commonly used in studies of the brain, cannot be effectively used to examine the spinal cord because of magnetic susceptibility artefacts and its relatively low spatial resolution [1].

We have implemented a DWI sequence in which echo collection is performed after the application of diffusion gradients in the same manner as the single-shot fast spin-echo technique, one of the fast imaging sequences [4]. We hypothesised that this technique could be applied to assessment of the normal cervical spinal cord and assess diffusion abnormalities in myelomalacia.

Materials and methods

Using a 1.5-tesla imager, we performed DWI with our new sequence in healthy volunteers (four men and two women aged 25–38 years) and 12 patients, eight men and four women, aged 34–86

years diagnosed on conventional images as having myelomalacia due to chronic compression of the cervical cord. The diagnosis of myelomalacia was made the basis of clinical and MRI findings at least two years prior to the DWI examination. The patients' lesions showed slight to moderate low signal on T1-weighted and high signal on T2-weighted images, but none showed marked signal change suggestive of a cyst. The patients' neurological status had been stable and of other pathology had been excluded clinically. When the volunteers were examined, a 3 cm-diameter plastic tube, filled with pure water and placed just behind the neck, was also imaged.

Like conventional single-shot fast spin-echo techniques, the DWI sequence collected 128 echoes after applying a 90–180 ° excitation pulse combined with a pair of diffusion gradients (Fig. 1). However, the sequence employed a data collection method in which the k-space was filled starting from its central line and continuing in each (plus and minus) direction. Other scanning parameters were: TE 80–100 ms; echo space 6 ms; imaging matrix 128×128; field of view 30×30 cm; section thickness 5 or 6 mm; one excitation; and imaging time 1 min 30 s. We did not employ the zero-filling method, a rectangular field of view, a reduced scan percentage, or a spatial saturation band. We also did not use cardiac gating or respiratory compensation. In the volunteers, we obtained axial and sagittal images of the cervical spinal cord with diffusion gradients of 423–488 s/mm^2 applied in three directions and calculated the apparent diffusion coefficients (ADC) on a pixel-by-pixel basis. In the patients, we performed multiple-slice imaging that yielded three sagittal images in which diffusion gradients of 400 s/mm^2 were applied in the craniocaudal direction. This was selected because on the volunteers' sagittal images the spinal cord showed high signal, probably due to the corticospinal tract when diffusion gradients were applied in the anterior-posterior or right-left directions. We did not include axial DWI in our assessment, as we obtained axial images in only six patients. We attached more importance to sagittal images, in which an entire lesion was seen in a single section. ADC maps were also created in all 12 patients to precisely assess changes in diffusion, because we did not think "T2 shine-through" was completely eliminated. Regions-of-interest for the ADCs were set manually on the console to include only the normal spinal cord in the volunteers and only the lesions in the patients. We selected values of b of 400–488 s/mm^2 as, in a previous evaluation, they consistently provided clinically acceptable images as regards signal-to-noise ratio and imaging time.

Two experienced neuroradiologists reviewed images from the volunteers and patients independently. They assessed the appearance of the normal cord and of lesions. The signal intensity of areas of myelomalacia was compared with that of the normal part of the cord. In cases of disagreement between the readers, the final judgment was reached by consensus.

Results

The spinal cord was well seen in all subjects, without the image distortion that is usually thought to be associated with echo-planar DWI. In the volunteers, the spinal cord gave high signal when diffusion gradients were applied in the anterior-posterior or right-left direction (Figs. 2 and 3). ADC maps were judged to be of adequate quality on visual assessment. It was possible to obtain ADC in all subjects by placing regions-of-interest. The calculated ADC for the cervical cords of the volunteers were 2.26 ± 0.08 and $2.13 \pm 0.36 \times 10^{-3}$ mm^2/s (mean ± SD) on the sagittal and axial images with diffusion gradients applied in the craniocaudal direction. The ADC of the spinal cord and water phantom with diffusion gradients in all directions n the anterior-posterior and right-left directions are shown in Table 1. Differences in the ADC from the phantom with the three encoding directions were not statistically significant (Student's t test, $P > 0.05$).

In patients with myelomalacia, the lesions appeared on DWI as areas of low signal (seven patients) or were isointense (five patients), and their ADC was 3.22 ± 0.26 and $3.37 \pm 0.42 \times 10^{-3}$ mm^2/s, respectively ($3.30 \pm 0.38 \times 10^{-3}$ mm^2/s overall). These values were significantly higher than those of the volunteers (Student t test, $P < 0.05$) (Fig. 4). Therefore, even lesions which were isointense on DWI, possibly due to partial volume effect,

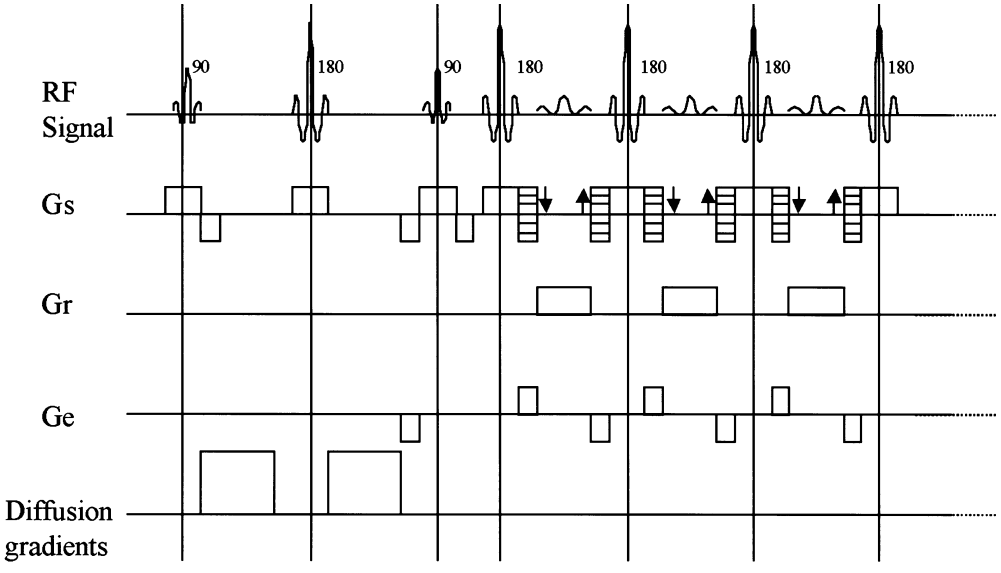

Fig. 1 Diagram of our sequence for diffusion-weighted imaging (DWI)

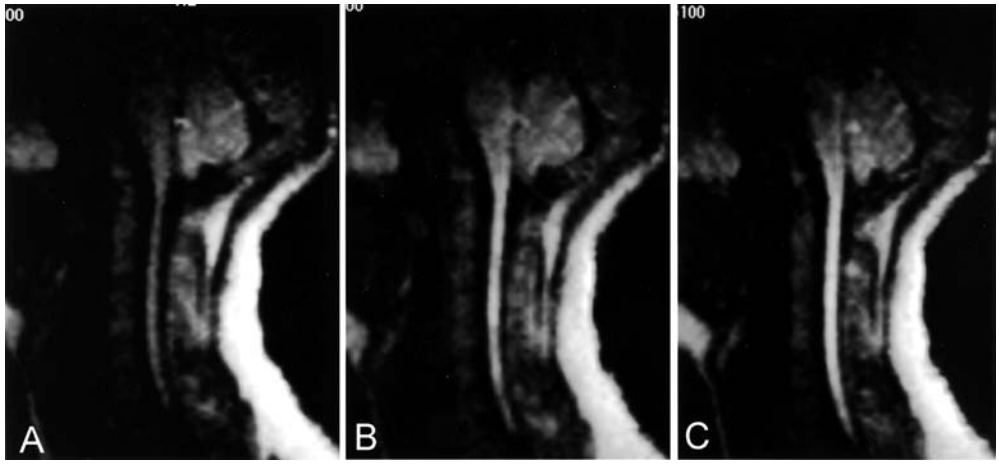

Fig. 2A–C Sagittal diffusion-weighted images of the cervical cord obtained from a volunteer. Diffusion gradients (b 423–488 s/mm^2) applied in **A** craniocaudal **B** anterior–posterior and **C** right–left directions. The cord gives high signal in **B** and **C**

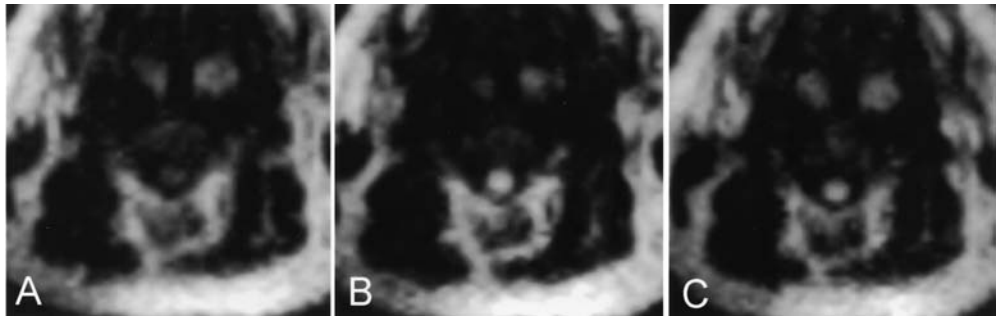

Fig. 3A–C As Fig. 2. The spinal cord again give high signal with diffusion gradients applied in the anterior–posterior and right–left directions. Grey matter and white matter cannot be distinguished

Table 1 Apparent diffusion coefficients cervical spinal cord and a water phantom

Direction of diffusion gradients	Craniocaudal (mean ± SD, $\times 10^{-3}$ mm^2/s)	Anterior-posterior (mean ± SD, $\times 10^{-3}$ mm^2/s)	Right-left (mean ± SD, $\times 10^{-3}$ mm^2/s)
Cervical spine (sagittal)	2.26 ± 0.08	1.54 ± 0.28	1.29 ± 0.52
Cervical spine (axial)	2.13 ± 0.36	0.82 ± 0.33	0.72 ± 0.32
Water phantom (sagittal)	2.42 ± 0.04	2.43 ± 0.04	2.37 ± 0.11
Water phantom (axial)	2.82 ± 0.16	2.76 ± 0.24	2.79 ± 0.12

were shown to have increased diffusion. Based on the DWI findings we informed neurosurgeons and orthopaedic surgeons that the lesions were likely to be irreversible. There were three patients who were imaged after decompression surgery. They had shown little clinical improvement and DWI 2.5, 3 and 3.5 years after surgery, respectively, showed increased diffusion within the lesions (Fig. 5).

Discussion

DWI is accepted as a robust technique for investigation of acute cerebral ischaemia. Its capability to assess water proton mobility has been said to be of clinical value in the diagnosis of brain lesions including infectious diseases, neoplasms, demyelinating diseases, trauma and metabolic diseases. DWI might also be useful for the diagnosis of similar conditions in the spinal cord. In the acute phase, spinal cord infarcts might be demonstrated on earlier on DWI than on conventional MRI, although spinal cord ischaemia is far less common than cerebral infarcts. DWI might also be expected to show diffusion abnormalities in the early phase of contusion, myelitis or plaques of multiple sclerosis.

Obtaining DWI of the spine is difficult for reasons mentioned previously. Several new MRI techniques have been reported, including a line-scanning technique, a navigated pulsed-gradient-echo technique and a radial-scanning technique [1, 2, 3]. Our technique uses a single-shot fast spin-echo technique which has also been described elsewhere [5]. Although this is not as fast as

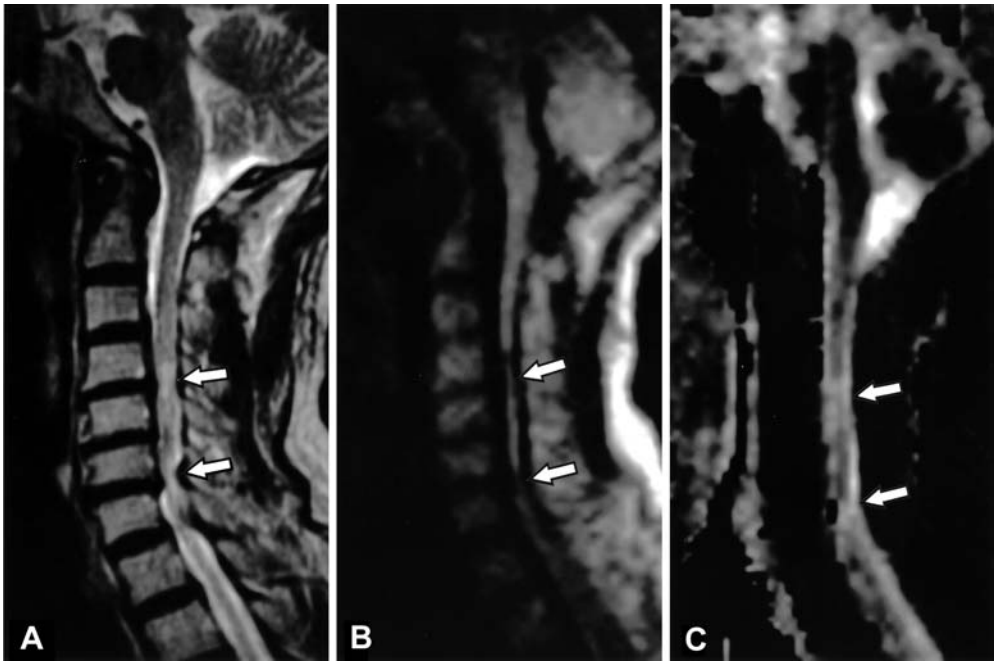

Fig. 4A–C Myelomalacia in a 71-year-old man. **A** A sagittal T2-weighted image shows high-signal myelomalacia caused by canal stenosis (*arrows*). **B** DWI with diffusion gradients (b 400 s/mm^2) applied in the craniocaudal direction reveals low-signal lesions (*arrows*). **C** The apparent diffusion coefficient (ADC) map shows that diffusion is increased in the lesions (*arrows*). These findings strongly suggested that the cord was irreversibly damaged, and the patient was accordingly treated conservatively

echo-planar imaging, it enabled us to acquire DWI without the need for cardiac gating or respiratory compensation. Unlike conventional fast spin-echo techniques, our sequence employed a data-collection method in which the k-space is filled starting from its centre. This made it possible to use an effective TE as short as 80–100 ms. Theoretically, a short effective TE can improve the signal-to-noise ratio, resulting in improved image quality [6, 7]. By starting data acquisition from the centre of k-space, reconstructed images appear smooth, although some blurring is also possible. T2 decay during the echo train can lead to blurring of the images [5] because data for the peripheral part of k-space which affects spatial resolution is collected at the end of the echo train.

Our results indicate that this technique can be used to generate both sagittal and axial DWI and ADC maps without degradation from motion or magnetic susceptibility artefacts. To our knowledge, only a few reports of axial in-vivo DWI of the spine in humans or experimental animals have been published [8, 9, 10]. However, our technique is limited by its spatial resolution: our in-plane spatial resolution was 2.34 mm. We could not, therefore, discriminate grey and white matter on the sagittal or axial images. Improving our technique would help to assess diffusion abnormalities in each of these areas. The signal-to-noise ratio, which we did not quantitate in this study, may not have been adequate.

Nevertheless, our technique was adequate to produce images showing the anisotropy of the normal spinal cord and diffusion abnormalities associated with myelomalacia due to chronic compression. Although the number of patients was small, we could detect significant increase in ADCs within areas of myelomalacia. On sagittal images of the patients, partial-volume effects caused by cord atrophy and rather thick sections may have been present. Obtaining axial DWI routinely may further improve the accuracy of assessing diffusion abnormalities within the spinal cord.

Myelomalacia is pathologically known to be composed of varying degrees of cystic necrosis of the central grey matter, syrinx formation and atrophy [10]. Therefore, the increased ADCs probably represent free proton mobility in areas of myelomalacia and its irreversibility. Further investigation comparing ADC values with disability might reveal the value of DWI in assessing function as well as indications for surgery on compressive lesions showing spinal cord high signal on conventional T2-weighted images. We believe that neurological and DWI findings in the three patients examined postoperatively support this assumption. Although we examined only patients with myelomalacia, the results suggest that our technique is efficacious for assessment of diffusion abnormalities in cervical cord lesions; it may be extended to acute cord ischaemia, myelitis of various causes, intramedullary neoplasms and demyelinating diseases such as multiple sclerosis.

The ADC of the cervical cord were similar to but slightly higher than those in previous reports [2, 9]. The ADC of the volunteers on sagittal and axial images showed considerable change when diffusion gradients were applied in the anterior-posterior and right-left directions. We have not as yet determined the reason for this. In addition to the volunteers in this study, we have

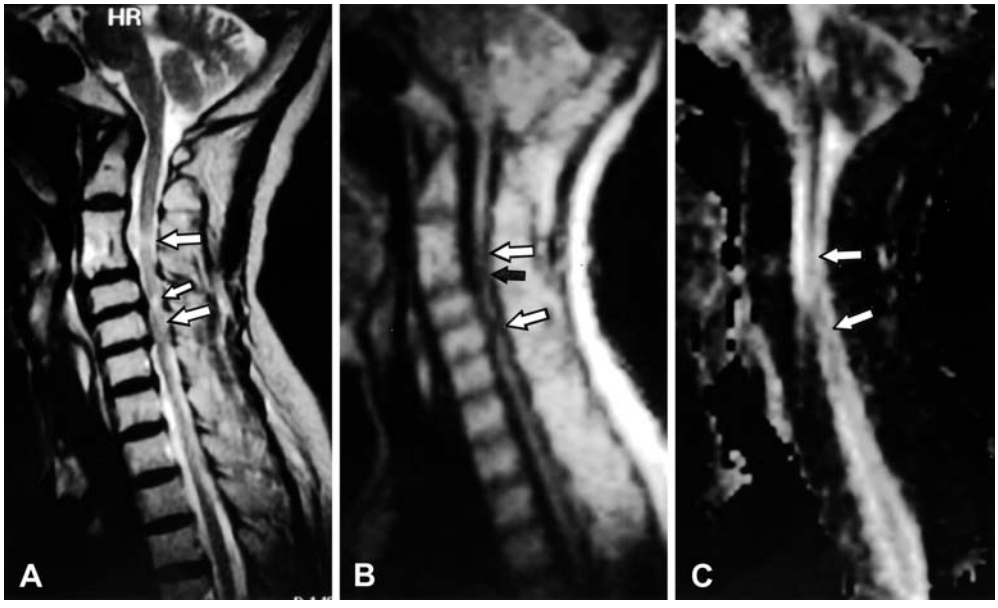

Fig. 5A–C Myelomalacia in a 67-year-old woman 3 years after decompressive surgery for the canal stenosis due mainly to ossification of the posterior longitudinal ligament at C3–6, most prominent at C3–4. **A** A T2-weighted image shows C3–4 anterior fusion and high signal indicating myelomalacia at C3–4 and C5–6 (*large arrows*). **B** DWI with diffusion gradients (b 400 s/mm^2) applied in the craniocaudal direction shows that the lesions of myelomalacia give low signal (*white arrows*). **C** This is confirmed as due to increased diffusion on the ADC map (*arrows*). Little improvement after surgery may partly be due to residual stenosis at C5–6, but the myelomalacia at C3–4, more extensive than at C5–6 was thought to be the main cause. Low signal at the C4–5 level (**B**, *black arrow*) may be partial-volume artefact. The high-signal area at C5–6 in **A** (small arrow), possibly representing recent vasogenic oedema, does not give low signal on DWI

also calculated ADC using sagittal images obtained with b 100 and 200 s/mm^2 in three other volunteers, yielding values of 1.72 and 1.69×10^{-3} mm^2/s. We assume that artefacts on the images obtained with a zero b, probably due to pulsation of the CSF, were the main cause of the difference. We plan to perform further studies to clarify this issue.

References

1. Robertson RL, Maier SE, Mulkern RV, Vajapayam S, Robson CD, Barnes PD (2000) MR line-scan diffusion imaging of the spinal cord in children. AJNR 21: 1344–1348
2. Clark CA, Barker GJ, Tofts PS (1999) Magnetic resonance diffusion imaging of the human cervical spinal cord in vivo. Magn Reson Med 41: 1269–1273
3. Dietrich O, Herlihy A, Dannels WR, et al (2001) Diffusion-weighted imaging of the spine using radial k-space trajectories. MAGMA 12: 23-31
4. Hennig J, Nauerth A, Friedburg H (1986) RARE imaging: a fast imaging method for clinical MR. Magn Reson Med 3: 823–833
5. Alsop DC (1997) Phase insensitive preparation of single-shot RARE: application to diffusion imaging in humans. Magn Reson Med 38: 527–533
6. McKinnon GC (1993) Ultrafast interleaved gradient-echo-planar imaging on a standard scanner. Magn Reson Med 30: 609–616
7. Holder CA (2000) MR diffusion imaging of the cervical spine. Magn Reson Imaging Clin N Am 8: 675–86
8. Schwartz ED, Yezierski RP, Pattany PM, Quencer RM, Weaver RG (1999) Diffusion-weighted MR imaging in a rat model of syringomyelia after excitotoxic spinal cord injury. AJNR 20: 1422–1428
9. Holder CA, Muthupillai R, Mukundan S Jr, Eastwood JD, Hudgins PA (2000) Diffusion-weighted MR imaging of the normal human spinal cord in vivo. AJNR 21: 1799–1806
10. Ramanauskas WL, Wilner HI, Metes JJ, Lazo A, Kelly JK (1989) MR imaging of compressive myelomalacia. J Comput Assist Tomogr 13: 399–404